

# Pulsar winds: transition to a force free regime

Z. Osmanov<sup>1</sup>, D. Shapakidze<sup>2</sup> and G. Machabeli<sup>3</sup>

E. Kharadze Georgian National Astrophysical Observatory

Received \_\_\_\_\_; accepted \_\_\_\_\_

arXiv:0711.0295v2 [astro-ph] 29 Jan 2008

---

<sup>1</sup>z.osmanov@astro-ge.org

<sup>2</sup>d.shapakidze@astro-ge.org

<sup>3</sup>g.machabeli@astro-ge.org

## ABSTRACT

The problem of reconstruction of the pulsar magnetospheres nearby the light cylinder surface is studied. It is shown that, on the basis of the Euler, continuity and induction equations, there is a possibility of parametrically excited rotational energy pumping process into the drift modes. As a result, the toroidal component of the magnetic field increases very rapidly. The increment is analyzed for plasma parameters of a typical pulsar magnetosphere. The feedback of the excited waves on the particles is considered to be insignificant. The dynamics of the reconstruction of the pulsar magnetosphere is studied analytically. It is traced from the generation of a toroidal component of the magnetic field up to transformation of the field lines into such a configuration, when plasma particles do not experience any forces: the motion of the particles switches to the so called force-free regime. At this stage the generation of the toroidal component comes to the end, and the pulsar wind reaches its stationary state.

*Subject headings:* pulsars, instabilities, plasma

## 1. Introduction

One of the major problem for pulsar winds concerns the transition of the magnetized plasma flows through the so called 'light cylinder' surface - a hypothetical zone, where the linear velocity of rotation equals to the speed of light. It is well known that the Goldreich & Julian current (Goldreich & Julian 1969) provides very strong magnetic field,  $B = 10^{12}G$ , leading to the co-rotation of the plasma flow within the pulsar magnetospheres. Generated magnetic field affects the dynamics of particles due to the centrifugal acceleration. This problem has been extensively studied in the series of works: Abramowicz & Prasanna (1990) considered the dynamics of a particle moving around the Schwarzschild black hole. It was shown that under certain conditions the centrifugal force changes its sign. Studying the simplest special relativistic case of kinematics of a test particle, moving along the straight co-rotating channel, Machabeli & Rogava (1994) revealed that the centrifugal force reversal if the particle velocity exceeds  $c/\sqrt{2}$  ( $c$  is the speed of light). A concrete astrophysical application of the centrifugal acceleration for the pulsar emission theory was considered by Gangadhara (1996). The author presents the centrifugal acceleration of the charged particles as the efficient mechanism producing high energy emission for millisecond pulsars. Recently, Osmanov et al. (2007a) have investigated the problem concerning TeV energy blazars, where the authors have found that the co-rotation of plasma particles provides high energy of relativistic electrons, which, in turn, guarantees TeV energies for soft photons via the inverse Compton scattering.

Generally speaking, no physical system can maintain the co-rotation in the nearby zone of the light cylinder surface. Therefore, the modification of the plasma stream dynamics is required. The plasma particles co-rotate with magnetic field lines in the vicinity of a pulsar's surface and flow outward. In order to provide the transition of the plasma outflow through the light cylinder surface, one needs to twist the field lines in a convenient manner.

In other words, the generation of a current, producing the toroidal component of the magnetic field, is necessary. Applying the special numerical methods, pulsar wind problem was studied in a series of works (Michel & Krause-Polstorff 1984; Krause-Polstorff & Michel 1985; Smith et al. 2001) and improved for 3D by Spitkovsky & Arons (2002) and Spitkovsky (2004). In these papers, the main assumption was the existence of an electric drift current producing the electromagnetic fields (Blandford 2002). In the present paper, we implement the method developed by Osmanov et al. (2007b) to investigate the influence of the *curvature drift* waves on the formation of magnetic field configuration.

Osmanov et al. (2007b) have found that even the small initial curvature of the magnetic field lines, resulting in a curvature drift current, may lead to the efficient formation of the toroidal component of magnetic field,  $B_r$ , due to the Curvature Drift Instability (CDI) (Kazbegi et. al 1989, 1991a,b; Shapakidze et. al 2003). As it has been shown by Osmanov et al. (2007b), the instability growth rate exceeds the slowdown rate of the pulsar rotation,  $\dot{P}/P$  (where  $P$  is a pulsar’s period), by many orders of magnitude. That indicates the existence of the natural mechanism providing the quick saturation of this process. Indeed, due to the CDI, the curvature of the magnetic field lines increases rapidly achieving the configuration when the plasma outflow has not taken the rotational energy off the pulsar any more. The transition of the plasma flow to the force-free regime will damp the instability. The study of the sweep back of the monopole and the dipole field lines due to the rotation is not novelty. In the papers by Michel (1973, 1974) the twisting of magnetic field lines was considered for the rotating axisymmetric multipole. It was quantitatively shown how the field lines make the transition from a closed to an open configuration in poloidal direction. However, the exact solution was not derived on the cusp of the light cylinder. The magnetic field lines formed perfect universal Archimedean spiral in the far field zone. For non axisymmetric force-free models, the problem was investigated in a series of papers: Mestel (1973) generalized the work developed in (Michel 1973), considering the

rotating pulsar frame of reference and found steady state solutions. The author suggested that the magnetic field lines emanating from the pulsar are trapped through the light cylinder surface. The force-free regime in the context of the pulsar emission theory has recently been studied by Gruzinov (2007). It has been shown that due to the force-free electrodynamics, the singular current layer is formed. The main bulk of the pulsar emission comes from this region.

The problem analysis handles well if one considers the mechanical analog of the motion of plasma flow along the pulsar magnetic field lines and studies the dynamics of a single particle motion inside the rotating channels. The kinematics of the relativistic motion of a bead along a linear, solid pipe rotating with constant angular velocity,  $\omega_0$ , was considered by Machabeli & Rogava (1994). As a consequence, the authors get an oscillatory motion of the bead along the pipe with a center in the rotation axis. In his part, de Felice (1995) examined the relativistic dynamics of a radially moving bead on the surface of a rigidly rotating disk. Authors arrive at the conclusion that the bead will never cross the light cylinder area relative to an inertial observer Chedia et al. (1996). The same mechanical problem, where the assumption of constant rotation is replaced by the more realistic set-up, was proposed by Machabeli et. al (1995). In this set-up "rotator+pipe+bead" device is considered to be a close system with finite initial energy and angular momentum. It was shown that the whole energy of the system finally transforms into that of the radially moving bead. Similarly to the previous work by Machabeli & Rogava (1994), the radial acceleration of the bead is negative in the area, where the rotation might be considered to be rigid. An alteration of its sign and corresponding rapid increment of the bead's velocity (or rapid decrement of the angular velocity  $\omega$ ) occurs within the light cylinder.

In Machabeli et al. (2000) the authors proposed to model the force-field of a rotating magnetic source as the differentially rotating medium (equivalent to a rotating and

permanently shape-variable "elastic pipe"). The model ensures the force-free motion of the particle along the "elastic pipe", so avoiding the problem of the light cylinder. Unlike this, in the present paper, we consider the co-rotating field lines and their possible deformation, in order to study the transition of the particle motion into the force-free regime.

We apply a method developed in (Rogava et al. 2003), where dynamics of a particle, moving along the co-rotating field lines, has been studied. It appears that in order to suppress the reaction force, the field lines, rather being straight, should deviate back and lag behind the rotation. Consequently, in due course of time, the curvature will increase, inevitably leading to decrement of the reaction force. This process will last until the magnetic field lines reach the configuration that vanishes the reaction force and stops their twisting.

In the present paper we consider the CDI as an efficient mechanism for reconstruction of magnetic field lines and investigate the transition of the plasma flow dynamics into the force-free regime.

The work is organized as follows: in section 2 we study the dynamics of particles moving, which provide the force-free regime. We derive the curvature drift instability growth rate and estimate the time scale of transition quasi straight magnetic field lines into the force free regime, in section 3 the corresponding results are present for typical values of pulsars and in section 4 we summarize the results.

## 2. Force-free kinematics

Let us prescribe the configuration of magnetic field lines with the Archimedes' spiral:

$$\Phi = aR, \tag{1}$$

where  $\Phi$  and  $R$  are the polar coordinates and  $a = \text{const}$  (see Fig. 1). Rogava et al. (2003) showed that the dynamics of the particle motion asymptotically tends to the force-free regime if the particle slides along the rotating channel having a shape of the Archimedes' spiral. However, in the Laboratory Frame (LF), the particle follows the straight linear paths with constant velocities. An observer from the LF will detect the following effective angular velocity:

$$\Omega_{ef} = \Omega + \frac{d\Phi}{dt} = \Omega + av, \quad (2)$$

where  $v$  is the particle velocity corresponding to the unit vector  $\mathbf{e}_R$  (see Fig. 1); and  $\Omega$  - the angular velocity of rotation. It is straightforward to show that, if the particle moves without acceleration in the LF, the corresponding effective angular velocity must be equal to zero. In this case Eq. (2) yields:

$$v = v_c \equiv -\frac{\Omega}{a}, \quad (3)$$

which means that, for each Archimedes' spiral with  $|a| > \Omega/c$  and  $a < 0$ , there exists a certain value of velocity,  $v_c$  (hereafter we call it "characteristic velocity"), when the LF trajectory of the particle is a straight line. The relativistic momentum of the particle writes as follows:

$$P_R = \gamma m v, \quad (4)$$

$$P_\Phi = \gamma m R \Omega_{ef}, \quad (5)$$

where  $\gamma$  is the particles' Lorentz factor.

The expansion of the equation of motion,  $d\mathbf{P}/dt = \mathbf{F}$  ( $\mathbf{F}$  is the reaction force), in terms of the corresponding components of the reaction force:

$$F_R = -\frac{aR}{\sqrt{1+a^2R^2}}|\mathbf{F}|, \quad (6)$$

$$F_\Phi = \frac{1}{\sqrt{1+a^2R^2}}|\mathbf{F}|, \quad (7)$$

yields the following equation (Rogava et al. 2003):

$$\frac{d^2 R}{dt^2} = \frac{\Omega - \gamma^2 v(a + \Omega v/c^2)}{\gamma^2 \Delta^2} \Omega_{ef} R, \quad (8)$$

where

$$\Delta \equiv \left( 1 - \frac{\Omega^2 R^2}{c^2} + a^2 R^2 \right)^{1/2}.$$

Note that  $(d^2 R/dt^2) \equiv 0$ , when  $v = -\Omega/a$ .

Since we are interested in relativistic flows, let us consider  $v_c = c$  setting  $a = -\Omega/c$ . In Figure 2 we show the dependence of  $\beta_R \equiv v/c$  versus  $R/R_c$  ( $R_c$  is the light cylinder radius) for the different initial values of  $\beta_{R0}$ . As it is clear from these plots, even though the initial velocity of particles is weakly relativistic (e.g.  $\beta_{R0} = 0.01$ ), it will asymptotically tend to the characteristic velocity,  $v_c$ . As a result, the particle trajectory in the LF must become linear.

Indeed, in Figure 3 we show the particle trajectory in the Rotational Frame (RF) of reference (see Fig.3a) as well as in the LF (see Fig.3b) for  $\beta_{R0} = 0.01$  and for the same spiral configuration with  $a = -\Omega/c$ . Observing the particle trajectory from the LF, one can notice that the path asymptotically becomes linear, indicating the conversion of the particle motion to the force-free regime. Therefore, we conclude that the magnetic field having the shape of the Archimedes' spiral may guarantee the transition of the plasma flow through the light cylinder surface.

In the next section we consider the possible plasma mechanism for twisting the quasi straight magnetic field lines in the magnetosphere.

### 3. Curvature drift instability

We start our consideration initially supposing that the magnetic field lines are almost straight with very small non zero curvature (see Fig. 4a).



The plasma stream is supposed to be moving along the co-rotating field lines provided by the strong magnetic field ( $\sim 10^{12}G$  for typical pulsars). We assume that the plasma flow is composed of two components: the plasma component ( $pl$ ) and, the so called, beam component ( $b$ ). The dynamics of plasma particles moving along the straight rotating magnetic field lines is described by the Euler equation (Machabeli et al. 2005)

$$\frac{\partial \mathbf{p}_\alpha}{\partial t} + (\mathbf{v}_\alpha \nabla) \mathbf{p}_\alpha = -\gamma_\alpha \xi \nabla \xi + \frac{e}{m} (\mathbf{E} + \mathbf{v}_\alpha \times \mathbf{B}), \quad (9)$$

where  $\xi \equiv \sqrt{1 - \Omega^2 l^2 / c^2}$ ;  $l$  is the coordinate along the straight field lines;  $\alpha = \{pl, b\}$  denotes the sort of particles;  $\mathbf{p}_\alpha$ ,  $\mathbf{v}_\alpha$ ,  $e$  and  $m$  are the momentum, the velocity, the charge and the rest mass of electrons, respectively;  $\mathbf{E}$  is the electric field and  $\mathbf{B}$  is the magnetic field. On the right hand side of Eq. (9) there are two major terms, from which the first represents the centrifugal force and the second - the Lorentz force. The full set of equation for  $n$ ,  $\mathbf{v}$ ,  $\mathbf{p}$ ,  $\mathbf{E}$  and  $\mathbf{B}$  should be completed by the continuity equation:

$$\frac{\partial n_\alpha}{\partial t} + \nabla(n_\alpha \mathbf{v}_\alpha) = 0, \quad (10)$$

and the induction equation:

$$\nabla \times \mathbf{B} = \frac{1}{c} \frac{\partial \mathbf{E}}{\partial t} + \frac{4\pi}{c} \sum_{\alpha=pl,b} \mathbf{J}_\alpha, \quad (11)$$

where  $n_\alpha$  and  $\mathbf{J}_\alpha$  are the density and the current, respectively.

Rewriting the Euler equation for the leading state and taking into account the frozen-in condition:  $\mathbf{E}_0 + \mathbf{v}_{0\alpha} \times \mathbf{B}_0 = \mathbf{0}$ , Eq. (9) reduces to Eq. (8). It is shown that for the ultra relativistic particles, pulling out the axis of rotation, the solution writes as (Machabeli & Rogava 1994):

$$v_{0\phi} \equiv v_{\parallel} = c \cos(\Omega t), \quad (12)$$

where  $v_{\parallel}$  denotes the velocity component along the magnetic field lines.

In due course of time, the centrifugal force causes the separation of charges in plasma consisting of several species. This process becomes so important that the corresponding electromagnetic field affects the dynamics of charged particles. Therefore, the produced electric field should also be considered in the Euler equation (9) as the next term of approximation (Osmanov et al. 2007b).

To make mathematics tractable we will linearize the set of Eqs. (9-11), supposing that in the zeroth approximation the flow has the longitudinal velocity satisfying Eq. (12). But due to the curvature, the flow is also drifting along the  $x$ -axis (see Fig. 4):

$$u_\alpha = \frac{\gamma_{\alpha 0} v_\parallel^2}{\omega_B R_B}, \quad (13)$$

where  $u_\alpha$  is the drift velocity,  $\omega_B = eB_0/mc$ ;  $R_B$  is the curvature radius of magnetic field lines; and  $B_0$  - the magnetic induction in the leading state.

Let us represent all physical quantities as sum of the zeroth and the first order terms:

$$\Psi \approx \Psi^0 + \Psi^1, \quad (14)$$

where

$$\Psi \equiv \{n, \mathbf{v}, \mathbf{p}, \mathbf{E}, \mathbf{B}\}.$$

Then expressing the perturbed quantities as follows:

$$\Psi^1(t, \mathbf{r}) \propto \Psi^1(t) \exp[i(\mathbf{k}\mathbf{r})], \quad (15)$$

examining only the  $x$  components of Eqs. (9,11) and bearing in mind that  $v_\parallel^1 \approx cE_x^1/B_0$  and  $k_\phi \ll k_x$ , one can easily reduce the set of Eqs. (9-11) to the following form:

$$\frac{\partial p_{\alpha x}^1}{\partial t} - i(k_x u_\alpha + k_\phi v_\parallel) p_{\alpha x}^1 = \frac{e}{c} v_\parallel B_r^1, \quad (16)$$

$$\frac{\partial n_\alpha^1}{\partial t} - i(k_x u_\alpha + k_\phi v_\parallel) n_\alpha^1 = i k_x n_\alpha^0 v_{\alpha x}^1, \quad (17)$$

$$-ik_\phi c B_r^1 = 4\pi e \sum_{\alpha=pl,b} (n_\alpha^0 v_{\alpha x}^1 + n_\alpha^1 v_\parallel). \quad (18)$$

Introducing a special ansatz for  $v_{\alpha x}^1$  and  $n_\alpha^1$ :

$$v_{\alpha x}^1 \equiv V_{\alpha x} e^{i\mathbf{k}\mathbf{A}_\alpha(t)}, \quad (19)$$

$$n_\alpha^1 \equiv N_\alpha e^{i\mathbf{k}\mathbf{A}_\alpha(t)}, \quad (20)$$

where

$$A_{\alpha x}(t) = \frac{u_\alpha t}{2} + \frac{u_\alpha}{4\Omega} \sin(2\Omega t), \quad (21)$$

$$A_{\alpha\phi}(t) = \frac{c}{\Omega} \sin(\Omega t) \quad (22)$$

and substituting Eq. (19,20) into Eqs. (16,17), one gets following expressions:

$$v_{\alpha x}^1 = \frac{e}{m\gamma_{\alpha 0}} e^{i\mathbf{k}\mathbf{A}_\alpha(t)} \int^t e^{-i\mathbf{k}\mathbf{A}_\alpha(t')} v_\parallel(t') B_r(t') dt', \quad (23)$$

$$n_\alpha^1 = \frac{ien_\alpha^0 k_x}{m\gamma_{\alpha 0}} e^{i\mathbf{k}\mathbf{A}_\alpha(t)} \int^t dt' \int^{t''} e^{-i\mathbf{k}\mathbf{A}_\alpha(t'')} v_\parallel(t'') B_r(t'') dt''. \quad (24)$$

Combining Eqs. (23,24) with Eq. (18), it is straightforward to reduce it into the form:

$$\begin{aligned} -ik_\phi c B_r^1(t) &= \sum_{\alpha=pl,b} \frac{\omega_\alpha^2}{\gamma_{\alpha 0}} e^{i\mathbf{k}\mathbf{A}_\alpha(t)} \int^t e^{-i\mathbf{k}\mathbf{A}_\alpha(t')} v_\parallel(t') B_r(t') dt' + \\ &i \sum_{\alpha=pl,b} \frac{\omega_\alpha^2}{\gamma_{\alpha 0}} k_x u_\alpha e^{i\mathbf{k}\mathbf{A}_\alpha(t)} \int^t dt' \int^{t''} e^{-i\mathbf{k}\mathbf{A}_\alpha(t'')} v_\parallel(t'') B_r(t'') dt''. \end{aligned} \quad (25)$$

Here  $\omega_\alpha = e\sqrt{4\pi n_\alpha^0/m}$  is the plasma frequency. For simplifying Eq. (25), one can use the following identity:

$$e^{\pm ix \sin \Omega t} = \sum_s J_s(x) e^{\pm is \Omega t}, \quad (26)$$

then Eq. (25) reduces to:

$$B_r(\omega) = - \sum_{\alpha=pl,b} \frac{\omega_\alpha^2}{2\gamma_{\alpha 0} k_\phi c} \sum_{\sigma=\pm 1} \sum_{s,n,l,p} \frac{J_s(g_\alpha) J_n(h) J_l(g_\alpha) J_p(h)}{\omega + \frac{k_x u_\alpha}{2} + \Omega(2s+n)} \times$$

$$\begin{aligned}
& \times B_r (\omega + \Omega (2[s - l] + n - p + \sigma)) \left[ 1 - \frac{k_x u_\alpha}{\omega + \frac{k_x u_\alpha}{2} + \Omega(2s + n)} \right] + \\
& + \sum_{\alpha=pl,b} \frac{\omega_\alpha^2 k_x u_\alpha}{4\gamma_{\alpha 0} k_\phi c} \sum_{\sigma, \mu=\pm 1} \sum_{s, n, l, p} \frac{J_s(g_\alpha) J_n(h) J_l(g_\alpha) J_p(h)}{\left( \omega + \frac{k_x u_\alpha}{2} + \Omega(2[s + \mu] + n) \right)^2} \times \\
& \times B_r (\omega + \Omega (2[s - l + \mu] + n - p + \sigma)), \tag{27}
\end{aligned}$$

where

$$g_\alpha = \frac{k_x u_\alpha}{4\Omega}, h = \frac{k_\phi c}{\Omega}.$$

Let us consider the resonance condition, which corresponds to the curvature drift modes. As it is clear from Eq. (27), the proper frequency for the CDI is:

$$\omega_0 \approx -\frac{k_x u_\alpha}{2}. \tag{28}$$

Therefore, physically meaningful solutions relate the case, when  $k_x u_\alpha/2 < 0$ . The present condition implies that  $2s + n = 0$  and  $2[s + \mu] + n = 0$ . On the other hand, one can easily check that for the typical quantities  $\gamma_b \sim 10^6$ ,  $\lambda \sim 6 \times 10^{10} \div 3 \times 10^{11} \text{ cm}$  (where  $\lambda \approx \lambda_x$  is the wave length) of *1-second pulsars* one gets  $|k_x U_{\alpha x}/2| \sim (0.02 \div 0.1) s^{-1}$  (here, it is supposed that  $k_x < 0$  and  $U_{bx} > 0$ , otherwise the resonance frequency would be negative). Note, that this value is much less than  $\Omega(2s + n)$  and  $\Omega(2[s + \mu] + n)$  for non vanishing  $s$  and  $n$ . Consequently, the corresponding terms become rapidly oscillative and their contribution tends to zero. Therefore, preserving only the leading terms of Eq. (27) (also taking into account that the beam components exceed the corresponding plasma terms by many orders of magnitude), one gets the dispersion relation for the CDI (Osmanov et al. 2007b):

$$\left( \omega + \frac{k_x u_b}{2} \right)^2 \approx \sum_{\sigma=\pm 1} \sum_{\mu=0, \pm 1} \sum_{s, l} \Xi_\mu J_s(g_b) J_{-2(s+\mu)}(h) J_l(g_b) J_{-2l+\sigma}(h), \tag{29}$$

$$\Xi_0 = 2\Xi_{\pm 1} = \frac{\omega_b^2 k_x u_b}{2\gamma_{b0} k_\phi c}. \tag{30}$$

In order to find the instability growth rate,  $\Gamma$ , let us write  $\omega \equiv \omega_0 + i\Gamma$  and substitute to Eq. (29). Then the growth rate of the CDI takes the following form:

$$\Gamma \approx \left[ \sum_{\sigma=\pm 1} \sum_{\mu=0,\pm 1} \sum_{s,l} \Xi_{\mu} J_s(g_b) J_{-2(s+\mu)}(h) J_l(g_b) J_{-2l+\sigma}(h) \right]^{\frac{1}{2}}. \quad (31)$$

Now we can qualitatively analyze, how the shape of magnetic field lines changes with time. After perturbing the magnetic field in the transverse direction, in due course of time, the toroidal component will grow and at some point a configuration of field lines will reach the shape of the Archimede's spiral. As we have already seen, the field lines with this shape guarantee the crossing of the light cylinder area by plasma particles and our objective will be to estimate the corresponding time scale when the field lines take the shape of the Archimede's spiral.

Referring to Figure 4b one has  $\tan \theta = B_r/B_{\phi}$  (the angle between the radius-vector of a point of the pipe and the tangent to the same point), on the other hand it is easy to show that  $\tan \theta = ax_{\phi}$ , then one gets:

$$\frac{B_r}{B_{\phi}} = ax_{\phi}. \quad (32)$$

Let us consider the toroidal component of magnetic field, as it behaves with time:

$$B_r \approx B_{0r} e^{\Gamma t}, \quad (33)$$

where  $t$  is time and  $B_{0r}$  - the initial perturbed value of the toroidal component.

Then taking into account the fact that we study the relativistic particles ( $a = -\Omega/c$ ) close to the LC surface ( $x_{\phi} \approx R_c$ ), from Eq. (32) one can get the corresponding time scale of the described process:

$$T \approx \frac{1}{\Gamma} \ln \left( \frac{B_{\phi}}{B_{0r}} \right). \quad (34)$$

As we see from Eq. (34) the time scale is a continuously increasing function of the

ratio  $B_\phi/B_{0r}$ . This is natural, because for bigger ratios the initial perturbation are smaller and consequently the magnetic field lines need more time to achieve the required structure.

#### 4. Discussion

Let us study the dependence of the time scale versus the wave length for several values of initial perturbations  $B_{0r}$ . In Figure 5 we show the behaviour of  $T(\lambda_x)$  considering several cases:  $B_\phi/B_{0r} \equiv \xi \in \{10; 10^3; 10^5; 10^7\}$ . As it is clear from these plots, the time scale is a linearly increasing function of the wave length.

The reconstruction of the magnetic field requires a certain amount of energy, therefore it is essential to estimate pulsar's slowdown luminosity ( $L_p$ ) and compare it to the "magnetic luminosity" ( $L_m \equiv \Delta E_m/T$ ). For  $L_p$  one has:

$$L_p = I\Omega\dot{\Omega} = I\frac{4\pi^2}{P^2}\frac{\dot{P}}{P}, \quad (35)$$

where  $I \sim MR_p^2$  is the moment of inertia of the pulsar,  $M \sim M_\odot \approx 2 \times 10^{33}g$  and  $R_p \sim 10^6 cm$  pulsar's mass and radius respectively. one can see that for typical pulsars:  $\dot{P}/P \sim 10^{-15}s^{-1}$  the slowdown luminosity is given by:

$$L_p \approx 7.9 \times 10^{31} erg/s. \quad (36)$$

The "magnetic luminosity" corresponding to the energy gain for  $\lambda_x \sim 2.5 \times 10^{11} cm$  ( $T \approx 10^3 s$ ) can be estimated straightforwardly:

$$L_m = \frac{B_r^2}{4\pi T}\Delta V, \quad (37)$$

where  $\Delta V \sim R_c^2 \Delta R = R_c^3 \varepsilon$  ( $\varepsilon \equiv \Delta R/R_c \ll 1$ ) is the volume, where the process of twisting takes place. Since we are studying the instability in the nearby zone of the LC, the magnetic field components must be given properly:  $B_\phi \sim \delta \times B_r = \delta \times B_p(R_p/R_c)^3$ , where

$\delta$  specifies the initial non dimensional perturbation of the toroidal component.  $B_p \sim 10^{12}G$  is the magnetic field near the pulsar's surface. Substituting all quantities into Eq. (37), and bearing in mind Eqs. (33,34), one can show that for  $\varepsilon \sim 0.1$  and  $\delta \sim 0.1$  the "magnetic luminosity" is given by:

$$L_m \approx 7.3 \times 10^{25} erg/s. \quad (38)$$

A direct comparison of Eqs. (39,40) exhibits:  $L_m \ll L_p$ , meaning that the magnetic field uses about  $\sim 0.0001\%$  of the total energy budget and therefore there is enough energy, to produce the required magnetic field.

In Figure ?? we show the behaviour  $T(\lambda_x)$  for the Crab pulsar for different initial perturbations. The dependence qualitatively does not change, the twisting process changes only quantitatively and as it is clear, the corresponding time scale is of the order of  $\sim 10^2s$ . Let us consider the energy budget corresponding to  $\lambda_x = 7 \times 10^6 cm$ . Then taking into account the derived value of the time scale:  $T \approx 30s$  (see Fig. ??), from Eq. (37) one can show that for  $\varepsilon = 0.1$  and  $\delta = 0.1$  the "magnetic luminosity" equals:

$$L_m^{Crab} \approx 6.8 \times 10^{31} erg/s. \quad (39)$$

On the other hand a direct calculation of the Crab pulsar ( $P \approx 0.033s$ ) luminosity, estimated by Eq. (35) gives:

$$L_p^{Crab} \approx 9.3 \times 10^{38} erg/s, \quad (40)$$

therefore also in the case of the Crab pulsar, the energy required for the reconstruction of the magnetosphere is  $\sim 0.00001\%$  of the pulsar's energy and the twisting process becomes feasible.

Generally speaking, in order to estimate how efficient is the instability, one has to compare its characteristic time scale to the corresponding time scale  $P/\dot{P}$ , characterizing the pulsar's slowdown rate. As observations show, this ratio ranges from  $10^{11}s$  (PSR 0531

- Crab pulsar) to  $10^{18}s$  (PSR 1952+29). But the highest twisting time scales shown in Figures 5,?? are of the order of  $10^4s$  and  $10^2s$  respectively, which are less by many orders of magnitude than  $P/\dot{P}$ . Therefore the sweepback mechanism is extremely efficient and may provide the reconstruction of magnetic field lines in such a way, that the dynamics becomes force-free and it is possible for plasma particles to avoid the light cylinder problem and go through the LC zone.



## 5. Summary

1. Examining the pulsar magnetospheric relativistic plasma, we have studied the role of the curvature drift instability in the process of sweepback of magnetic field lines.
2. Making the linear analysis of the Euler, continuity and induction equations, we have derived the dispersion relation governing the curvature drift instability.
3. Considering the resonance frequencies of the sweepback process, an expression of the instability increment has been obtained.
4. Based on the expression of the instability growth rate, we have derived the formula of the transition time scale of quasi linear configuration of field lines into the Archimedes' spiral, guaranteeing the force-free regime.
5. The transition time scale has been studied versus the wave length for the typical *1-second* pulsars and the Crab pulsar. For both cases it was shown that the corresponding time scale is less than pulsar's spin down rates by many orders of magnitude indicating high efficiency of the present process.

The research was supported by the Georgian National Science Foundation grant GNSF/ST06/4-096.

## REFERENCES

- Abramowicz, M. A. & Prasanna, A.R., 1990, MNRAS, **245**, 729
- Blandford R.D., 2002, luml. conf., **381B**
- Chedia, O.V., Kahniashvili, T.A., Machabeli, G.Z., & Nanobashvili, I.S., 1996, Ap& SS **239**, 57
- Felice de, F., 1995, Phys.Rev, **A52**, 3452
- Gangadhara, R. T. 1996, A&A, 314, 853
- Goldreich, P. & Julian, W.H., 1969, ApJ, 157, 869
- Gruzinov A., 2007, ApJ, **667**,L69
- Kazbegi A.Z., Machabeli G.Z. & Melikidze G.I., in *Joint Varenna-Abastumani International School & Workshop on Plasma Astrophysics*, volume ESA SP-285, edited by T.D. Guyenne, (European Space Agency, Paris, 1989), p. 277
- Kazbegi A.Z., Machabeli G.Z. & Melikidze G.I., 1991a, MNRAS, **253**, 377
- Kazbegi A.Z., Machabeli G.Z. & Melikidze G.I., 1991b, Aust. J. Phys. **44**, 573.
- Machabeli, G.Z., Nanobashvili, I.S. and Rogava, A.D., 1995, Izv. Vuz. Radiofizika, **39**, 34
- Machabeli, G.Z. & Rogava, A. D., 1994, Phys.Rev. A, 50, 98
- Machabeli G., Osmanov Z. & Mahajan S., Phys. Plasmas 12, 062901 (2005)
- Machabeli G.Z., Mchedlishvili G.Z., & Shapakidze D.E., 2000, Ap&SS, **271**, 277
- Mestel L., 1973, Ap& SS, **24**,289
- Michel F. Curtis, 1972, ApJ, **180**,207

- Michel F. Curtis, 1974, ApJ, **187**,585
- Michel F.C. & Krause-Polstorff J., 1984, MNRAS, **213**, 43
- Krause-Polstorff J. & Michel F.C. , 1985, A&A, **144**, 72
- Osmanov, Z. Rogava, A. & Bodo, G., 2007a, A&A, 470, 395O
- Osmanov, Z., Dalakishvili, Z. & Machabeli, Z. 2007b, MNRAS, 383, 1007
- Rogava, A. D., Dalakishvili, G. & Osmanov, Z.N., 2003, Gen. Rel. and Grav. 35, 1133
- Shapakide, D., Machabeli, G. Melikidze, G., & Khechinashvili, D., 2003, Phys.Rev.E, **67**, 026407
- Smith I.A., Michel F.C., Thacker P.D., 2001, MNRAS, **322**, 209
- Spitkovsky A., 2004, 'Young Neutron Stars and Their Environments, IAU Symposium no. 218, held as part of the IAU General Assembly, 14-17 July, 2003 in Sydney, Australia. Edited by Fernando Camilo and Bryan M. Gaensler. San Francisco, CA: Astronomical Society of the Pacific, 2004, p.357
- Spitkovsky A. & Arons J., 2002, ASP Conf. Ser., **271**, 81S
- Torres Diego F., & Nuza Sebastián E., 2002, ApJ, 583, L25

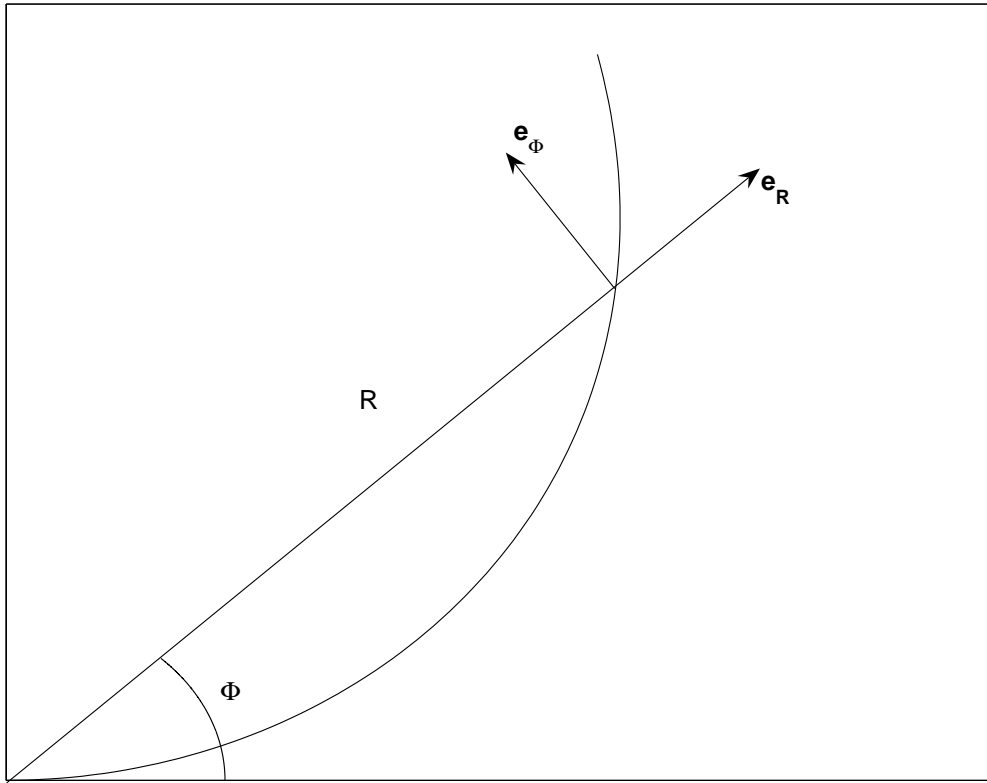


Fig. 1.— The Archimedes spiral in polar coordinates.

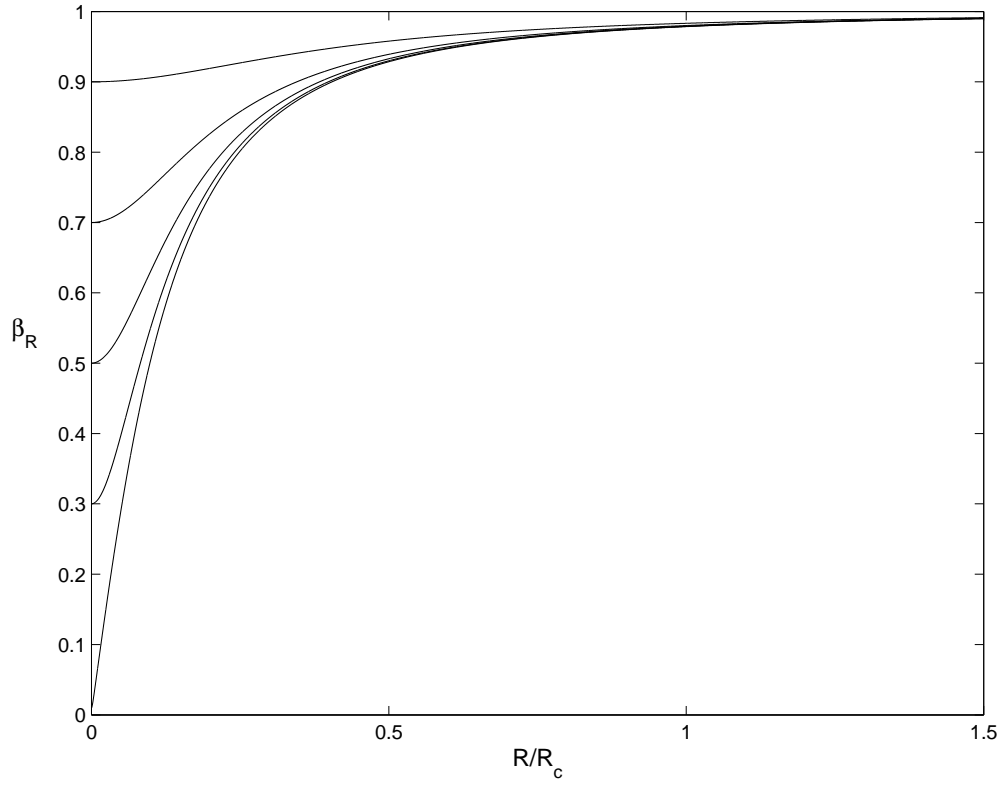


Fig. 2.— Behaviour of  $\beta_R$  versus  $R/R_c$ . The set of parameters is  $P = 1s$ ,  $\beta_{R0} = \{0.01; 0.3; 0.5; 0.7; 0.9\}$ .

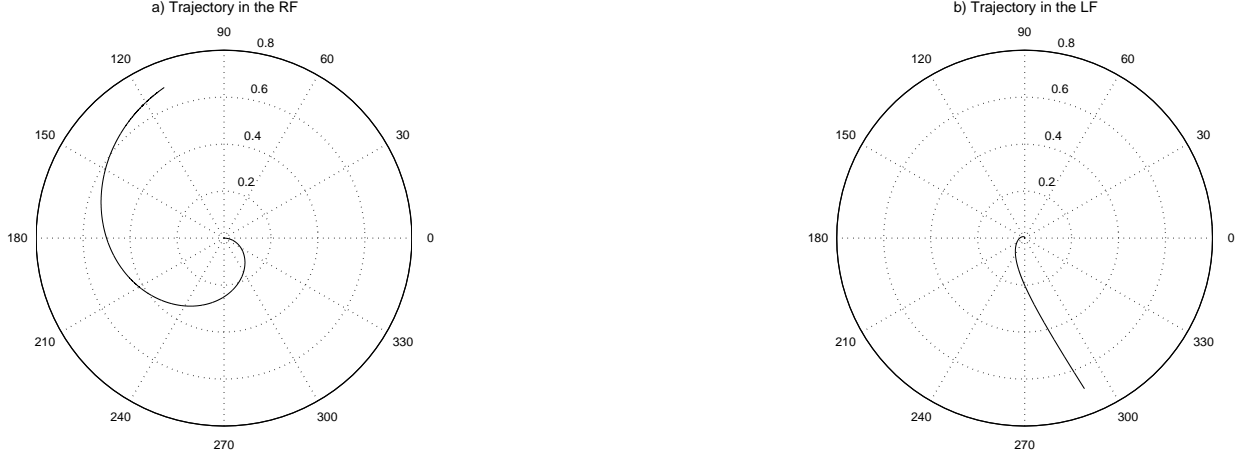


Fig. 3.— As it is seen from (b) when the RF trajectory of the particle is presented by the Archimedes spiral [see (a)], the LF trajectory asymptotically tends to the straight line configuration. The set of parameters is  $P = 1s$  and  $\beta_{R0} = 0.01$ .

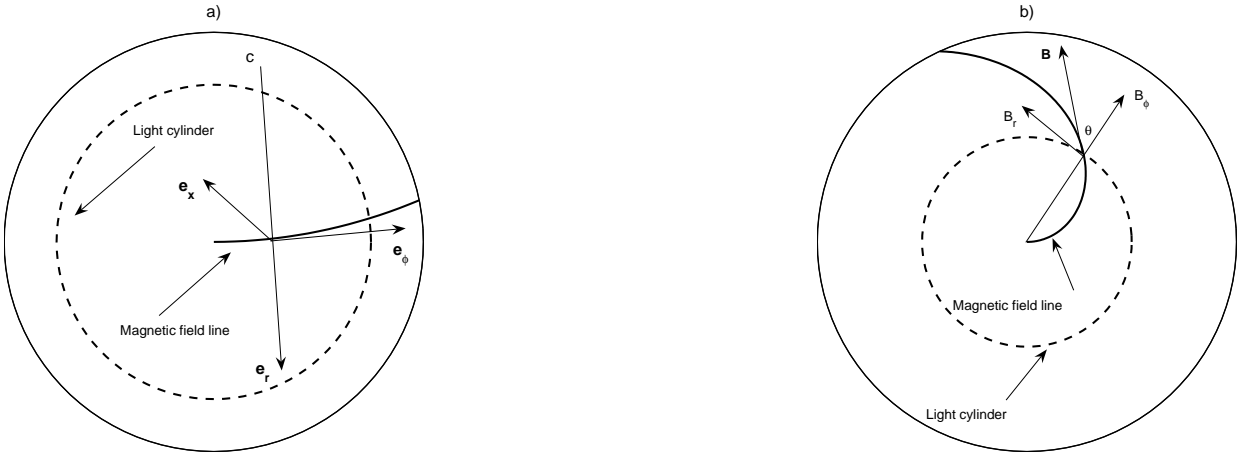


Fig. 4.— On (a) we show geometry in which we consider our system of equations. By  $\mathbf{e}_\phi$ ,  $\mathbf{e}_r$  and  $\mathbf{e}_x$  the unit vectors are denoted, note that  $\mathbf{e}_x \perp \mathbf{e}_{r,\phi}$ .  $C$  is the curvature center. On figure (b) we show geometry, which is necessary for derivation of Eq. (34).

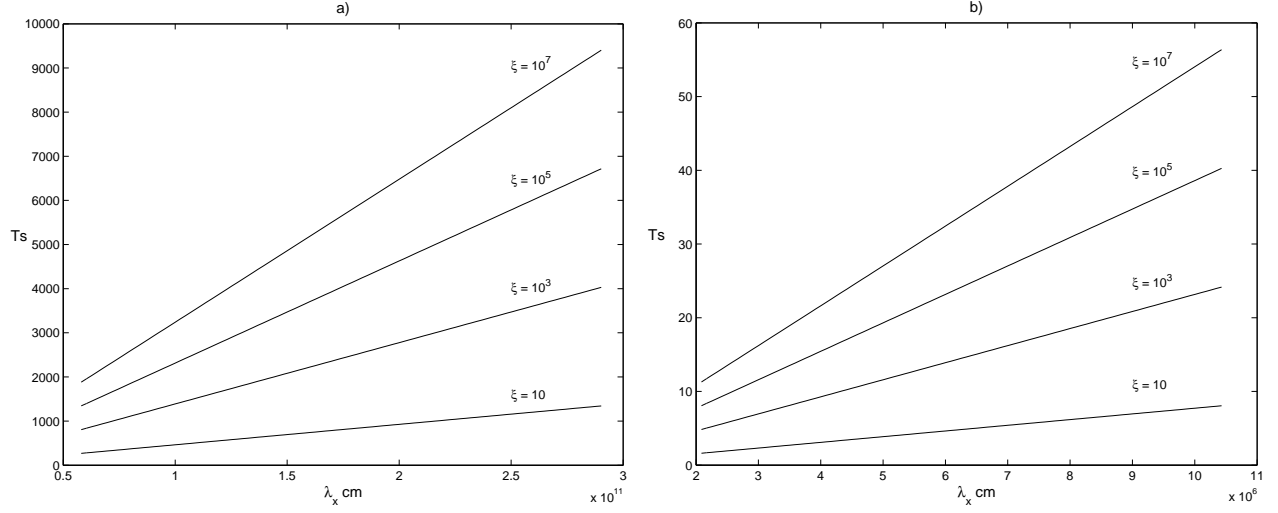


Fig. 5.— Here we show the behaviour of the time scale of sweepback of the magnetic field lines versus the wave length for the *1-second* pulsar [see (a)] and the Crab pulsar  $P \approx 0.033s$  [see (b)] respectively. The set of parameters is:  $\xi = \{10; 10^3; 10^5; 10^7\}$ ,  $\gamma_b \sim 10^6$ ,  $\lambda_x \approx \lambda$  and  $\lambda_\phi = 1000R_c$ .